EPJ manuscript No.
(will be inserted by the editor)

Particle-phonon coupling: understanding the variety of excitations in the low-lying spectra of odd nuclei

S. Leoni[1], A. Bracco[1], G. Colò[1], and B. Fornal[2]

[1] Department of Physics, University of Milano and INFN sez. di Milano, Via Celoria 16, 20133 Milano, Italy
[2] Institute of Nuclear Physics PAN, ul. Radzikowskiego 152, 31-342 Krakow, Poland

Received: date / Revised version: date

Abstract. The couplings between particles and vibrations in atomic nuclei play a key role in the understanding of several nuclear properties, as it has been highlighted along several decades. In this contribution, after a short survey of the early discoveries of particle-phonon multiplets around the ^{208}Pb region, we review recent experiments and theoretical attempts to understand low-energy spectra of odd-nuclei close to magic and semi-magic cores, where **polarization** phenomena play a significant role. The focus will be on nuclei around ^{48}Ca, ^{132}Sn, ^{208}Pb and neutron-rich Ni isotopes. Special emphasis will be given to experimental techniques based on high-resolution γ-spectroscopy and to recent theoretical developments aimed at disentangling particle-phonon coupled states and other more hybrid configurations, using the Hybrid Configuration Mixing model that has been recently proposed by the Milano group.

PACS. 21.60.-n Nuclear structure models and methods – 23.20.Lv gamma transitions and level energies – 27.40.+z $39 \leq A \leq 58$ – 27.60.+j $90 \leq A \leq 149$ – 27.60.+w $190 \leq A \leq 219$

1 Introduction

Although the states of the nuclear spectra should emerge in their full richness from large-scale shell model calculations, where all possible arrangements of the nucleons within a basis of mean-field orbitals are taken care of, the idea that there are specific "building blocks" that permit a clear understanding of these spectra has proven to be very instrumental since the early days of nuclear physics. In fact, nuclear excitations can have either a single-particle character or a collective character (in the case of vibrations or rotations of the nucleus as a whole) and shell-model cannot always predict vibrational or rotational states, and may have trouble also to predict other collective phenomena, such as clustering in nuclei (which is, however, outside the scope of this paper). As a result, it became rather natural to perceive that single particle excitations and collective states may actually be the aforementioned building blocks and describing nuclei in terms of these elementary excitations has been pursued extensively both by the Dubna group led by V.G. Solovev [1] and by the Copenhagen school under the influence of A. Bohr and B.R. Mottelson [2].

P.F. Bortignon was, together with R.A. Broglia, D.R. Bes and R. Liotta, one of the developers of the Nuclear Field Theory (NFT), based on the interplay between vibrational degrees of freedom (bosons) and single-particle or quasi-particle degrees of freedom (fermions). In the seminal work of Ref. [3], applications to the region around ^{208}Pb have been discussed: in particular, excited states in ^{209}Bi, observed in ^{209}Bi(d,d') and (t,α)^{210}Po reactions, have been interpreted, setting emphasis, in general terms, on the interplay between the states emerging from either inelastic scattering or transfer reactions. In this context, we deem relevant to mention also other early works that have elucidated the special role played, in the region around ^{208}Pb, by the coupling with the very collective 3^- (octupole) vibration [4], as well as with the pairing vibrational modes [5]. For instance, the multiplet made up in ^{209}Bi by the odd $h_{9/2}$ proton coupled with the 3^- phonon has been a remarkable testing ground.

Over the years, a large body of experimental work, often in parallel with increasingly more refined theoretical studies, has confirmed the relevance of the picture of atomic nuclei based on the interplay between fermionic and bosonic degrees of freedom. In this context, odd nuclei are of special interest, being sensitive to **terms in the nuclear force (time-odd terms) and to correlations** that simply do not show up in even-even systems. Here, we will limit ourselves to examples that pertain to the scope of this paper, namely to the discussions of nuclei one/two-particles away from magic cores. Such "simple" sysyems are of key importance **since fermion-boson couplings, in terms of particle-phonon couplings,** play a significant role. More particle-phonon multiplets than the one observed in ^{209}Bi have been partially identified experimentally and theoretically interpreted, in the mass regions around A=150 and 200 [6–10]. In a number of other works, the coupling between low-lying nuclear

vibrations, or phonons, and single-nucleon degrees of freedom has been recognised as a key ingredient for the understanding of a large variety of nuclear phenomena. We like to emphasise here the damping width of Giant Resonances, either based on the ground-state [11–13] or at finite temperature [14,15], and the anharmonicities displayed by double Giant Resonances [16] that have been subject of intense investigations in the 1990s [17].

From a broader perspective, coupling phenomena between fermions and collective excitations (bosons) are well known to occur in many-body systems in all branches of physics, starting from the emblematic cases in electronic systems: the electron-plasmon couplings in metals, or the electron-phonon couplings that give rise to superconductivity, are the counterparts of the couplings of nucleons with collective excitations [18]. Last but not least, it should be mentioned that P.F. Bortignon has co-authored papers [19,20] aimed at showing how the coupling between particles and vibration in atomic nuclei emerges from the general equations of the quantum theory of many-body Fermi systems.

Starting from the 1990s, it has become possible to develop particle-vibration coupling (PVC) models that start from microscopic Hamiltonians, e.g., of the Skyrme type [21]. This has been one of the constant interests of the Milano group, and in recent years these calculations have been implemented without approximations [22] and applied to different problems than those we have previously discussed, like charge-exchange Giant Resonances (cf. Ref. [23] but also the contribution by H. Sagawa *et al.* in the present volume) and β-decay [24]. The latest chapter of this story, that has still P.F. Bortignon among the main actors, concerns the so-called Hybrid Configuration Mixing Model (HCM) that has been introduced in Ref. [25].

The motivation for introducing the HCM model is strongly linked with experimental developments that have recently allowed to extend our understanding of low-lying nuclear spectra, with new assignments of spin and parities, and accurate electromagnetic transition probabilities, as we will discuss below in detail for a number of cases. Often, one finds spectra, in odd nuclei, where states with clear single-particle character, or members of a particle-phonon multiplet, coexist with states that have non-collective character. In order to deal with these situations, the HCM model has been conceived, and applied first to spectra in the neighbourhood of shell closures (yet being meant as a first step toward a comprehensive description of the spectra of heavy nuclei that are not easily accessible to shell model calculations [26,27]). Details of the model can be found in Refs. [25,28] while we limit ourselves to a short discussion of the formalism here (being our emphasis on the physics behind and the comparison with experimental data).

The HCM model is a self-consistent approach, with no adjustable parameters, in which both single-particle states and core excitations come out of Hartree-Fock (HF) and Random Phase Approximation (RPA) calculations, respectively, performed with the same Skyrme interaction. From RPA, not only collective states but also pure 1 particle-1 hole (1p-1h) states are extracted and kept: these will be alluded to, in what follows, as core excitations. As a consequence, the states of the odd nucleus are a mixture of particle plus phonon states and 2 particle-1 hole (2p-1h) states. In such a situation, one must take care of the fact that the basis is not orthonormal. We have used the technique of Ref. [29] to cope with this, and the work of Ref. [28] is full of details about the assessment of the effectiveness of such technique. While the HCM model is self-consistent, namely it is based on a microscopic Skyrme functional, the choice of the specific Skyrme set matters to some extent. In the results later discussed, we have picked up the Sly5 and SkX functionals, that display different values of the effective mass m^*/m.

The goal of this paper will be to show how experimental developments have been blooming lately and, to some extent, also how they have motivated the building of the HCM model, and what can be understood through the model (confronting obviously with other models like the shell-model or with *ab initio* calculations whenever available). The regions on which such recent experimental investigations of nuclear systems have been focusing are shown in the magnified panels of Fig. 1. In the text which follows, we will first consider the neutron-rich ^{61,65,67}Cu (Z=29) isotopes, which will highlight the role played by excitations based on the coupling of a single $p_{3/2}$ proton to the 3^- phonon of the corresponding Ni (Z=28) core. In these cases, the data interpretation will be based on a simple extension for the case of open-shell nuclei of the original particle-phonon weak-coupling model by A. Bohr and B.R. Mottelson [2]. The limitations of this approach will be briefly discussed.

Further experimental results, that call for extensions of the theory, will be then addressed. These concern nuclei consisting of one or two nucleons around a double-magic core, such as ^{48}Ca, ^{132}Sn or ^{208}Pb; these are the main double shell closures in the neutron-rich side of the nuclear chart and are also dispayed in Fig. 1. In particular, we will focus on ^{47}Ca, ^{49}Ca, ^{131}Sn, ^{133}Sb and ^{210}Bi, for which the Milano-Krakow collaboration has performed extensive experimental high-resolution gamma spectroscopy investigations, tacking advantage of high-efficiency Ge arrays and of suitable reactions induced by heavy ions, as well as by intense neutron beams. The interpretation of the data will be mainly based on the HCM model for nuclei around mass A=48 and A=132, as discussed in Section 2, and on Shell Model approaches in the case of mass A=208. In this latter case, the need for future developments of the HCM will be mentioned.

2 Experimental Investigation

2.1 Around the semi-magic Ni isotopic chain: the cases of ^{61,65,67}Cu

Neutron-rich Cu nuclei are ideal systems to study nuclear structure properties around the Z=28 proton-shell closure, having one proton only outside the Ni closed shell. In particular, information on the robustness of the proton shell

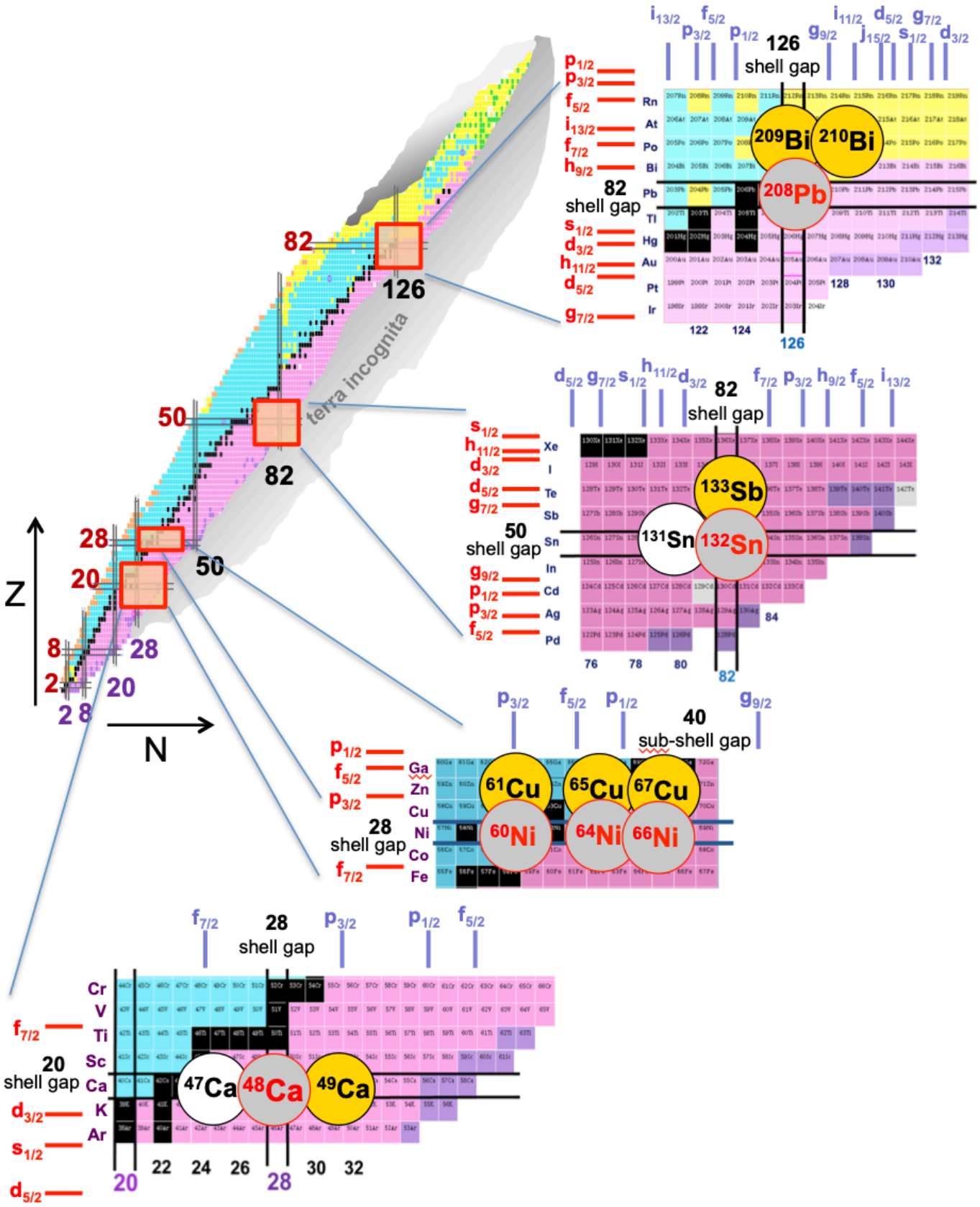

Fig. 1. Top Left: Pictorial view of the nuclear chart, indicating the stability valley (in black) and known unstable nuclei (β^+, β^- and α emitters in light blue, pink and yellow, respectively). The grey area shows the region of still unkown, unstable exotic nuclei expected to exist in the Universe, for a total of more than 7000 atomic nuclei. Proton and neutron shell closures are indicated by solid lines and labelled by the corresponding magic numbers. Left: Expanded regions around the ^{48}Ca, ^{132}Sn and ^{208}Pb neutron-rich doubly magic systems, and the semi-magic Ni neutron-rich isotopic chain. For each region of interest, single particle levels for protons and neutrons are given. Valence particle (hole) nuclei discussed in this work are highlighted in yellow (white).

closure may be obtained by the combined study of single- and few-particle excitations, as well as of states arising from the coupling of the unpaired $p_{3/2}$ proton to phonon excitations of the Ni core.

In the works of Refs. [30,31], our collaboration has investigated, both experimentally and theoretically, the nature of the $9/2^+$ states in ^{61}Cu, ^{65}Cu and ^{67}Cu, which were already known to show contradictory properties. In Fig. 2, a systematic survey of the spectra of $^{59-69}$Cu isotopes, in which the known properties of the $9/2^+$ excitations are highlighted (energy and γ-decay branching), is provided [32]. We also show the energies of the 3^- phonon states in the corresponding Ni isotopes (dashed lines).

As one can see, in all odd-mass Cu isotopes, the first $9/2^+$ states is found around 2.5 MeV. They have large spectroscopic factors as hinted by the (α,d) and (^{3}He,d) proton-stripping reactions data [33,34]. This is typical for states having mainly single-particle character. At the same time, (α,α'), (e,e') and (p,p') inelastic scattering data [35–39] give, at least in the case of ^{63}Cu and ^{65}Cu, a significantly large E3 strength for these states ($\approx$ 20 W.u.), that one would attribute to the coupling with the 3^- phonons of ^{62}Ni (B(E3) = 13(2) W.u.) and ^{64}Ni (B(E3) = 10(2) W.u.) [40], respectively. Candidates for the other members of the $\pi p_{3/2} \otimes 3^-$ multiplet were also observed at higher energies, above 3 MeV, in the excitation energy region where the 3^- phonons of Ni nuclei are located. To shed light on this complex scenario, lifetime measurements were performed for the $9/2^+$ states in ^{61,65,67}Cu, together with accurate measurements of the γ-decay branches to the $3/2^-$ ground states (that were not available in all cases). The experimental B(E3) values have been then compared with theoretical predictions based, in this case, on a revised version of the original particle-phonon weak-coupling model of A. Bohr and B.R. Mottelson [2].

The experiments were performed at the 9 MV Tandem accelerator of the Horia Hulubei National Institute of Physics and Nuclear Engineering (IFIN-HH) in Bucharest, and the nuclei of interest were populated by the reactions ^{48}Ti(^{16}O, p2n)^{61}Cu, ^{64}Ni(^{7}Li, α2n)^{65}Cu and ^{64}Ni(α,p)^{67}Cu, with beam energies of 54, 32 and 18 MeV, respectively. Gamma rays were detected using the mixed ROSPHERE setup [41], consisting of 14 HPGe detectors and 11 $LaBr_3$(Ce) scintillator detectors (for fast-timing measurements), with absolute detection efficiency of $\approx$1.5% and $\approx$1%, at 1.33 MeV. While the lifetime of the $9/2^+$ state in ^{61}Cu was obtained by using a plunger device, the lifetimes of the $9/2^+$ states in ^{65}Cu and ^{67}Cu were extracted using the fast-timing method, as reported in Refs. [30,31]. The experiments yielded the values τ = 4.3(7) ps, 37(3) ps and 227(22) ps, for the $9/2^+$ states in ^{61}Cu, ^{65}Cu and ^{67}Cu, corresponding to B(E3) values of 22(5), 9(2) and 17(2) W.u., respectively. In the analysis, accurate branching values were taken into account for the $9/2^+$ decay to the $3/2^-$ ground state: in the case of ^{61}Cu a branching of 2.5(4)% was measured, for the fist time, in the present experiment, while branching values for ^{65}Cu and ^{67}Cu were taken from Ref. [42].

As mentioned in the introduction, the Cu isotopes were among the first to be investigated by our collaboration, and the theoretical interpretation was based on an extension to open-shell nuclei of the weak-coupling particle-phonon model that is described at p. 425-430 of Ref. [2]. In this weak-coupling model, particle states $|j'm'\rangle$ and phonons $|LM\rangle$ are assumed to be known, and their couplings are taken into account by means of the lowest-order diagrams of perturbation theory. In particular, the shift of the energies of the members of the multiplet given by $|\,(j' \otimes L)_j\rangle$ can be calculated within second-order perturbation theory, as is clear by the diagrams (a-d) of Fig. 6-10 in [2]. Consistently, the electromagnetic transition probabilities can be calculated according to the detailed formulas of Ref. [4]. We have performed microscopic HF-BCS plus QRPA calculations of ^{64,66}Ni (cf. Refs. [43,44] for details), that provide single-particle and quasi-particle states (neutrons turn out to be superfluid while protons are not in the semi-magic Ni isotopes), together with the phonon states and in particular the collective 3^- states. Two different microscopic Skyrme parameter sets have been employed, namely SkX [45] and Sly5 [46]. For neutrons, a zero-range, density-dependent surface pairing interaction has been used, and its parameters have been fitted in order to reasonably reproduce the pairing gaps along the Ni isotopic chain in the region of interest.

The calculated $9/2^+$ state is found theoretically to be located slightly higher than the experiment, by 400-500 keV, in ^{65,67}Cu. In ^{61}Cu, by taking the energy of the 3^- core excitation from experiment, the agreement is better as we reach less than 200 keV difference. This would go in the direction of a $9/2^+$ state with a dominant component from the low-lying octupole phonon. However, the comparison between measured and calculated B(E3) values, shown in Fig. 3, clearly points to a more complex structure for the $9/2^+$ state. The simple picture of a single proton coupled to the octupole phonon in the corresponding Ni core seems to be at variance with the experimental findings in both ^{61}Cu and ^{67}Cu. This indicates a structure for the $9/2^+$ states in which contributions from other type of excitations could play a significant role. Indeed, results from recent spectroscopy works in the Ni neutron rich region point also to a rather complex scenario of coexistence of spherical, oblate and prolate shapes, in the excitation energy region below 4 MeV [47–50], thus suggesting the need for more refined theoretical interpretations.

2.2 Around the stable doubly-magic ^{48}Ca nucleus: the cases of ^{47,49}Ca

In the case of Ca nuclei, the neutron-rich isotope ^{48}Ca is doubly magic and exhibits only one sizable collective excitation, i.e. the 3^- phonon, located at 4.507 MeV, characterised by a fairly large value of the reduced electromagnetic transition probability, given by B(E3) = 6.8 $\pm$ 1 W.u. [51]. The first 2^+ state, at 3.832 MeV, shows instead no sign of collectivity, as its B(E2) value is smaller than 2 W.u. The collectivity of the 3^- excitation suggests the possible existence of clear multiplets of positive parity

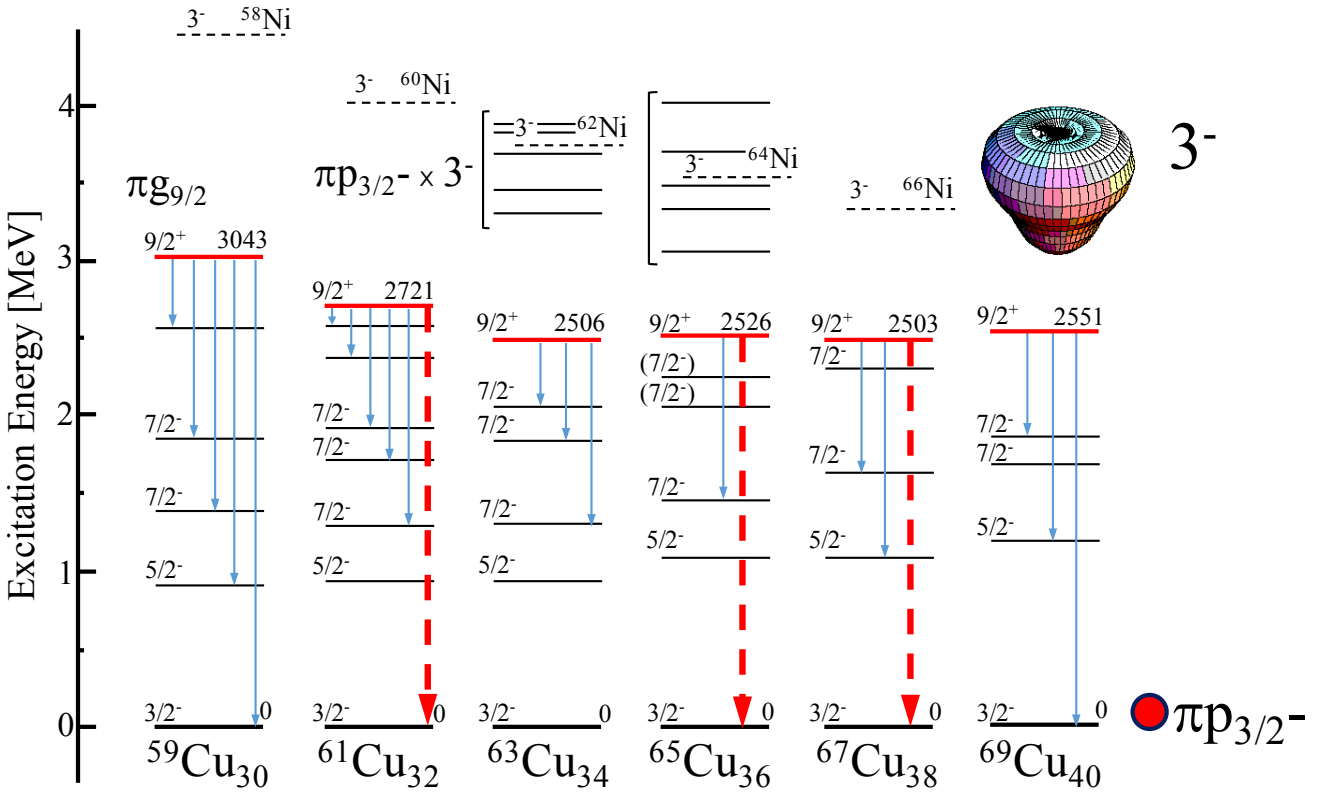

Fig. 2. Energy levels and γ-ray branchings for the first excited $9/2^+$ states in $^{59-69}$Cu isotopes. The 3^- octupole states in the corresponding Ni isotopes are indicated by dashed lines. In the case of ^{61,65,67}Cu, the lifetimes of the $9/2^+$ states (which are candidates for being $\pi p_{3/2}\otimes$Ni(3^-) coupled states) have been measured with the ROSPHERE array [41], using plunger and fast-timing techniques (see text for details) [30,31]. Thick-dashed arrows show the corresponding direct decay to the ground state, measured in ROSPHERE. (Adapted from Ref. [32]).

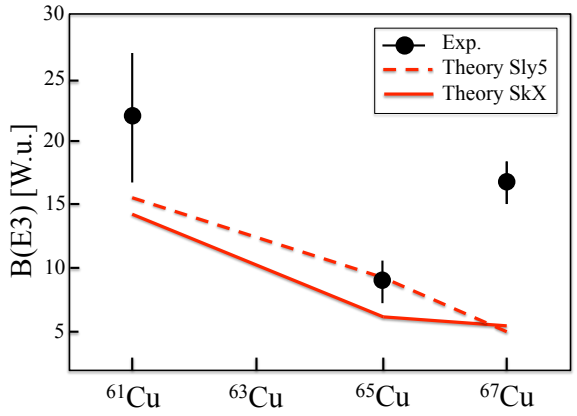

Fig. 3. Comparison of the experimental B(E3) transition probabilities and theoretical calculations, within the schematic Bohr and Mottelson particle-phonon coupling model, for the $9/2^+$ states in ^{61,65,67}Cu isotopes [30,31].

states, made up by the coupling of the 3^- with either the valence $p_{3/2}$ neutron in the case of ^{49}Ca or with the $f^{-1}_{7/2}$ neutron hole in the case of ^{47}Ca.

In recent experiments performed at the Legnaro National Laboratory of INFN (Padova, Italy) [52–54], firm spin and parity assignments, as well as lifetimes, have been obtained for states previously indicated as candidates for particle-phonon coupled structures [55,56]. The nuclei of interest were populated in heavy-ion transfer reactions, employing a ^{48}Ca beam at 6 MeV/u on thin ^{64}Ni and ^{208}Pb targets. The detection setup consisted in the large acceptance magnetic spectrometer PRISMA [57,58], combined with the high efficiency Ge array CLARA [59]. Figure 2 shows the decay scheme of ^{47}Ca and ^{49}Ca, as observed in the Legnaro experiment, together with the known 2^+ and 3^- excitations of ^{48}Ca [55]. Particle-phonon candidates are marked in red, and their decay is indicated by thick red arrows, while thin arrows refer to the decay from states having single-particle nature. The B(Eλ) values of the relevant γ transitions are reported in Weisskopf units (W.u.), and from these values one clearly sees that a fingerprint for states arising from the coupling with the collective 3^- phonon of ^{48}Ca is a large B(E3) value associated to the direct decay to the ground state, of similar magnitude as that of the 3^- phonon in ^{48}Ca. This is the case of the $9/2^+$ and $11/2^+$ states in ^{49}Ca and ^{47}Ca, respectively.

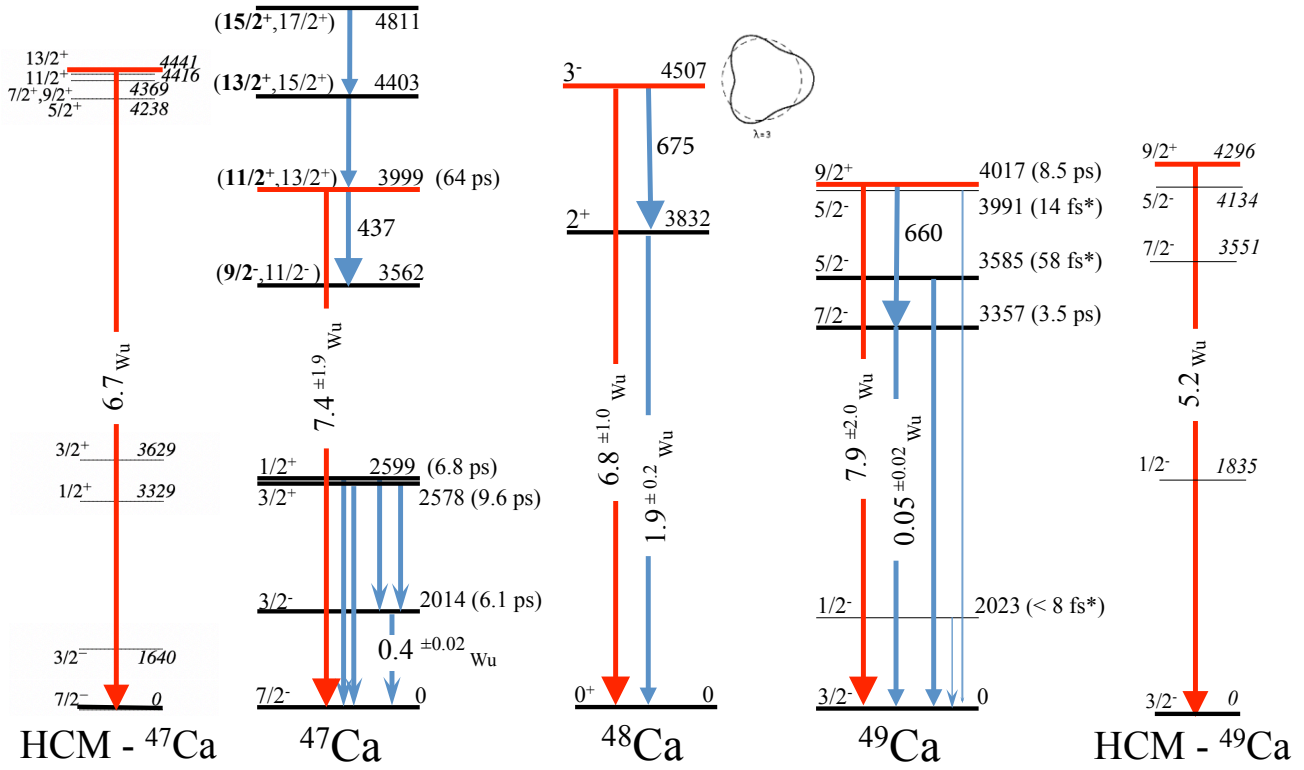

Fig. 4. Experimental level schemes of ^{47}Ca and ^{49}Ca, as observed in the heavy-ion transfer reactions of Ref. [52,54], together with the 2^+ and 3^- excitations of the ^{48}Ca core, known from literature [55]. On the left and right side, predictions for ^{47}Ca and ^{49}Ca from the Hybrid Configuration Mixing model are given.

Ca isotopes were the first to be interpreted by our collaboration on **the** basis of the Hybrid Configuration Mixing model. On the left and right side of Fig. 4, the excitation spectra of ^{47}Ca and ^{49}Ca, calculated with the Hybrid Configuration Mixing model, are shown for comparison. As we mentioned in the Introduction, this model is based on single-particle states $|j'm'\rangle$ and on core excitations $|LM\rangle$ but there are two differences with the Bohr and Mottelson weak-coupling model [2]:

- the interaction between particles and core excitations is diagonalized on the basis of the aforementioned states, and not treated within perturbation theory;
- the core excitations include all states below a given energy cutoff, regardless whether they are collective or not. The corrections associated with the fact that such a basis is not orthonormal are taken care of.

As in the case of Ni isotopes, we use a microscopic Skyrme Hamiltonian, and we start from HF single-particle states and core excitations that are calculated within self-consistent RPA. In the model, the Hamiltonian reads

$$\begin{aligned} H &= H_0 + V, \\ H_0 &= \sum_{jm} \epsilon_j a^\dagger_{jm} a_{jm} + \sum_{NJM} \hbar\omega_{NJ} \Gamma^\dagger_{NJM} \Gamma_{NJM}, \\ V &= \sum_{\substack{jm \\ j'm'}} \sum_{NJM} h(jm; j'm', NJM) a_{jm} [a^\dagger_{j'm'} \otimes \Gamma^\dagger_{NJM}]_{jm}. \end{aligned} \quad (1)$$

H_0 is the sum of the unperturbed HF and RPA Hamiltonians, namely $a^\dagger_{jm}$ is the creation operator of a HF single-particle (s.p.) state $|jm\rangle$ and ϵ_j is the corresponding energy, $\Gamma^\dagger_{JM}$ is the creation operator of a RPA excitation $|NJM\rangle$ and $\hbar\omega_{NJ}$ is its energy. V is the coupling between the s.p. states and the RPA excitations **and its matrix elements are written in detail, in terms of the X and Y RPA amplitudes, in Ref. [22]**. We stress that we use the same Energy Density Functional self-consistently, namely HF states and self-consistent RPA solutions are obtained using a given Skyrme set, and the same functional is used to determine the interaction V. Thus, no free parameter is introduced.

The basis on which we want to solve this Hamiltonian contains single-particle states $|jm\rangle$ as well as states of the type $|j'm' \otimes NJM\rangle_{jm}$ made up with particles that are coupled with low-lying RPA excitations. In practice, we select a finite number of these states $|i\rangle$ $(i = 1 \ldots n)$ and we write down the Hamiltonian matrix. However, the states of the basis do not form, in general, an orthonormal set. Thus, we must write the generalized eigenvalue problem,

$$(H - \mathcal{N}E)\,|\Psi\rangle = 0. \quad (2)$$

In the basis made up with the states $|i\rangle$, Eq. (2) becomes

$$\sum_j (H_{ij} - \mathcal{N}_{ij}E)\,|j\rangle = 0, \quad \forall i. \quad (3)$$

Here, $\mathcal{N}$ is the overlap matrix between the basis states, and we must pick up a technique to handle this equation by distinguishing the cases in which the determinant of $H - \mathcal{N}E$ vanishes while that of $\mathcal{N}$ does not, from the cases in which the determinant of $\mathcal{N}$ vanishes and spurious solutions must be eliminated. We do it by using the method introduced in Ref. [29].

Once we have solved the generalised eigenvalue problem and we have also the wave functions of the states at our disposal, various kinds of matrix elements can be calculated. Ref. [30] provides the detailed formulas for the calculation of the matrix elements of **multipole** transition operators.

In ^{49}Ca, the agreement with the experiment is satisfactory for the $9/2^+$ state, which is dominated by the coupling with the collective octupole phonon of the ^{48}Ca core, but also for the $5/2^-$ and $7/2^-$: the former shows a rather pure single-particle character while the latter has a main 2p-1h component. In ^{47}Ca the situation is instead more complex. The lowest $3/2^-$ state is found by theory to be rather mixed, with dominant configurations made by the coupling of the $f^{-1}_{7/2}$ neutron hole with the $f^{-1}_{7/2}p_{3/2}$ neutron excitations of the core. For what concerns the $f^{-1}_{7/2}\otimes 3^-$ multiplet (with spin $1/2^+$, $3/2^+$ ... $13/2^+$), the lowest members ($1/2^+$ and $3/2^+$) are found to exhibit a sizeable single-particle component, of the order of 30-40%, while the highest spin members, not all identified experimentally, are found to be very pure, with a B(E3) value in agreement with the data.

It is worth mentioning that ^{47}Ca and ^{49}Ca isotopes have been studied, in recent years, in a number of new experiments. Our collaboration has employed cold neutron capture reactions, at the Institut Laue-Langevin in Grenoble, to reach the most complete low-spin spectroscopy of such systems, from the ground state up to the neutron binding energy [61,62]. Indeed, several new transitions have been observed in both ^{47}Ca and ^{49}Ca, and the spectroscopy of ^{41}Ca was also largely extended [63]. Experiments have been also performed with the GRETINA segmented high-resolution γ-ray detection system [64] at NSCL, Michigan State University, by employing intermediate energy heavy-ion-induced neutron knockout [65] and neutron pickup reactions [66], with the aim of studying the relative spectroscopic strengths associated with high-l orbitals, as in the case of the $f^{-1}_{7/2}$ neutron hole in ^{47}Ca and ^{49}Ca, and of the $g_{9/2}$ and $f_{5/2}$ neutron orbitals in ^{49}Ca. In these works, data were compared with large scale shell-model calculations, performed using a truncated model space, and with shell-model calculations in the pf and $pfg_{9/2}$ model space, using **chiral NN+NNN interactions**. In general, theory predictions are satisfactory and in agreement with the HCM model, with some exceptions. The results depend in fact on the choice of the chiral force and the underlying reasons are not clear **(so far, results from calculations that employ different chiral forces are different even with respect to bulk properties like saturation of nuclear matter, binding energies etc.).**

2.3 Around the exotic doubly-magic ^{132}Sn nucleus: the one-proton nucleus ^{133}Sb and the one-neutron hole nucleus ^{131}Sn

The exotic doubly magic system ^{132}Sn displays three collective excitations (i.e., the 2^+, 3^- and 4^+ phonons) around 4-4.5 MeV, with a similar strength (about 7 W.u.) [55, 67,68]. As a consequence, nuclei in the vicinity of ^{132}Sn are expected to exhibit excited states arising from the coupling of these phonons to particle/hole states. In recent years, our collaboration has performed extensive γ-spectroscopy investigations on both ^{133}Sb [69] and ^{131}Sn [70], having one proton particle and one neutron hole with respect to the doubly magic ^{132}Sn core. Both systems are therefore ideal for testing shell model predictions, as well as approaches taking into account collective excitations of the core.

Experimental data were obtained during the EXILL campaign [71] at the PF1B cold-neutron facility at Istitut Laue Langevin (Grenoble, France), exploiting fission induced by a highly collimated cold neutron beam, with a capture flux of 10^8 neutrons s^{-1} cm^{-2}, impinging on thick ^{235}U and ^{241}Pu targets. High-resolution gamma spectroscopy data were obtained using an efficient HPGe ball, consisting of up to 46 crystals, the largest array ever used with an intense neutron beam. In addition, the use of a fully digital and triggerless acquisition system allowed the study of γ coincidences up to several tens of microseconds apart. With this setup, nuclei characterized by microsecond isomers, identified in previous works, could be studied in detail, extending the spectroscopic information above the isomeric states, as in the case of ^{133}Sb (having a 16.6 μs $21/2^+$ isomer, located at 4545 keV) and ^{131}Sn (having a 0.3 μs $23/2^-$ isomer, at 4605 keV).

Figure 5 shows a comparison between the experimental level scheme of the core nucleus ^{132}Sn (in the center), and those of ^{133}Sb and ^{131}Sn (on the right and left side of ^{132}Sn). New transitions observed during the EXILL campaign, above the long-lived isomers, are marked in red in both cases. In ^{133}Sb, high spin positive parity states have been interpreted, in previous works, as members of the multiplet arising from the coupling of the odd $g_{7/2}$ proton to the $f_{7/2}h^{-1}_{11/2}$ neutron excitation of the core. However, a more detailed comparison with theory has to take into account, in a general scheme, all relevant core excitations, including the ones associated with the collective 2^+, 3^- and 4^+ phonons of the core. A similar situation is expected in ^{131}Sn, with the unpaired $h^{-1}_{11/2}$ neutron hole.

Such comprehensive calculations have been performed in the framework of the Hybrid Configuration Mixing model approach, and the predicted excitation spectra are reported, for comparison, on the left and right side of Fig. 5. In both cases, states dominated by the couplings with the collective phonons of ^{132}Sn are found to appear in the 4-5 MeV excitation energy region, coexisting with states of less collective nature. In the case of ^{133}Sb, in particular, fast changes in the wave function compositions (e.g., from collective to less collective nature) are observed with increasing spins, as indicated by measured transition rates.

Indeed, the results of the calculations, in reasonable agreement with the data, clearly indicate the complexity of the structure of nuclei in the ^{132}Sn region, supporting the need for comprehensive theoretical approaches, similar to the HCM model, in which larger model spaces should also be explored.

2.4 Around the stable doubly-magic ^{208}Pb nucleus: the one-proton, one-neutron nucleus ^{210}Bi

Nuclei in the proximity of ^{208}Pb, one of the best known doubly-magic nucleus of the nuclear chart, are ideal candidates for testing interactions among valence particles, as well as excitations arising from the coupling with the very collective 3^- octupole phonon (at 2615 keV with B(E3) $\approx$ 34 W.u.). Indeed, ^{209}Bi, with one valence $h_{9/2}$ proton with respect to the ^{208}Pb core, is the first observed and only case, thus far, where the complete set of states arising from a phonon-particle coupling is known: they are the 7 members of the $h_{9/2}\otimes$ 3^- multiplet, with spins ranging from $3/2^+$ to $15/2^+$ [72]. As discussed in the Introduction to this paper, the experimental findings in ^{209}Bi triggered the original particle-phonon weak-coupling model of Bohr and Mottelson, followed by a series of works leading to a profound investigation and to an elegant theory to which Pier Francesco Bortignon has largely contributed. In other nuclei around ^{208}Pb, such as ^{206,209}Pb, ^{206,207}Tl and ^{206}Hg [9,8,10], states originating from couplings of the 3^- phonon with single particles/holes have been located as well, although mainly at the highest spins. In the case of ^{210}Bi, with one-valence-proton and one-valence-neutron with respect to the ^{208}Pb core, information on proton-neutron excitations and couplings of particles with excitations of the ^{208}Pb core are expected at the same time. The low-energy structure of ^{210}Bi, up to $\approx$ 2 MeV, is in fact only originating from couplings of a proton on the $1h_{9/2}$, $2f_{7/2}$, $1i_{13/2}$, $2f_{5/2}$, $3p_{3/2}$, $3p_{1/2}$ orbitals and a neutron on the $2g_{9/2}$, $1i_{11/2}$, $1j_{15/2}$, $3d_{5/2}$, $4s_{1/2}$, $2g_{7/2}$, $3d_{3/2}$ orbitals. At higher excitation energies, instead, states originating from the couplings between valence particles and the very strong 3^- octupole vibration of ^{208}Pb should appear.

The low spin structure of the ^{210}Bi nucleus has been recently studied, with high resolution, in a cold neutron capture experiment [73,74] performed during the EXILL campaign [71]. From the capture state, at 4605 keV, the decay of ^{210}Bi was found to proceeds through 64 primary gamma rays (40 observed for the first time), followed by several decay paths which populated a total number of 70 discrete states (33 newly found). Angular correlation analysis provided information on the multipolarity of the transitions and allowed to firmly establish spin-parity assignments for the majority of the states. Together with results from previous works [55], almost complete spectroscopy of ^{210}Bi, at low spins ($J \leq 8$), was achieved. As shown in Fig. 6, the experimental excitation spectrum of ^{210}Bi was then compared with shell model calculations performed with the OXBASH code [75] and the Kuo-Herling interactions [76], assuming the ^{208}Pb core as frozen. Below 3.5 MeV, a one to one correspondence was found between experimental states and calculated excitations of one-proton- and one-neutron-valence particles, apart from 12 observed states, which could not be assigned to the shell model predictions. It is very likely that such states, located between 2 and 3 MeV, originate from the coupling between the 2.6 MeV 3^- octupole phonon in ^{208}Pb, as observed in other nuclei of the same mass region. Theory work is ongoing to describe the structure of ^{210}Bi within the Hybrid Configuration Mixing model approach.

3 Conclusions

In this paper we have reviewed recent experiment and theory efforts devoted to the understanding of low-excitation energy spectra in odd nuclei, close to magic and semi-magic cores, focusing on the regions of ^{48}Ca, ^{132}Sn, ^{208}Pb and neutron-rich Ni isotopes. We have highlighted the importance of coupling mechanisms between particles and phonons in the description of complex excitations, also in the spirit of recalling the pioneering works on this topic that have been co-authored by Pier Francesco Bortignon.

In the light of recent high-precision γ-spectroscopy measurements, we have discussed the need for novel theory approaches which can describe, on equal footing, particle-phonon coupled states as well as other more hybrid configurations. This is the case of the Hybrid Configuration Mixing model, developed by the Milano theory group. Perspectives for future investigations in more complex systems are given, **including the case of superfluid nuclei and the extension to the case more than one particle outside the core**, following the "red thread" always indicated to us by Pier Francesco. His legacy and guidance will always have a profound impact on the scientific activities carried out in our groups.

This work was supported by the Italian Istituto Nazionale di Fisica Nucleare and by the Polish National Science Centre under Contracts No. 2014/14/M/ST2/00738, 2013/08/M/ST2/0 and 2016/22/M/ST2/00269.

References

1. V.G. Soloviev, *The Theory of Atomic Nuclei: Quasiparticles and Phonons* (Institute of Physics Publishing, Bristol and Philadelphia, 1975).
2. A. Bohr, B.R. Mottelson, *Nuclear Structure. Vol. II* (W.A. Benjamin, New York, 1975).
3. P.F. Bortignon, R.A. Broglia, D.R. Bes and R. Liotta, Phys. Rep. 30, 305 (1977).
4. I. Hamamoto, Phys. Rep. 10, 63 (1974).
5. P.F. Bortignon, R.A. Broglia, D.R. Bes, R. Liotta, V. Paar, Phys. Lett. B64, 24 (1976).
6. P. Kleinheinz, Physica Scr. 24, 236 (1981).
7. P. Kleinheinz et al., Phys. Rev. Lett. 48, 1457 (1982).
8. N. Pietralla et al., Phys. Lett. B681, 134 (2009).
9. M. Rejmund et al., Eur. Phys. J. A8, 161 (2000).
10. B. Fornal et al., Phys. Rev. Lett. 87, 212501 (2001).

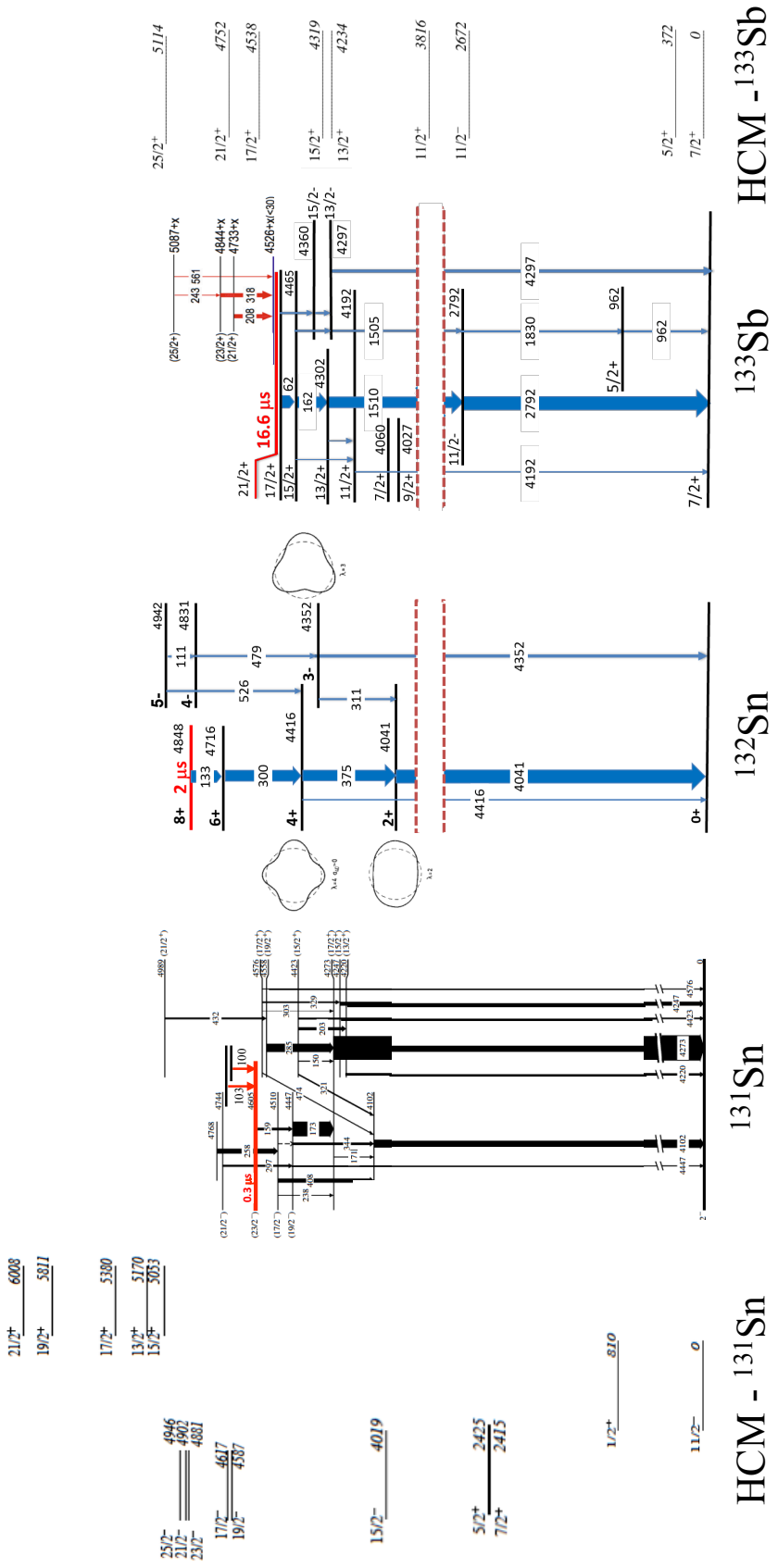

Fig. 5. Experimental excitation spectra of ^{131}Sn, ^{132}Sn and ^{133}Sb. Long lived isomeric states are marked in red, as well as new transitions feeding the isomers, recently observed by our collaboration [69,70]. On the left and right side, predictions by the HCM model are given for ^{131}Sn and ^{133}Sb.

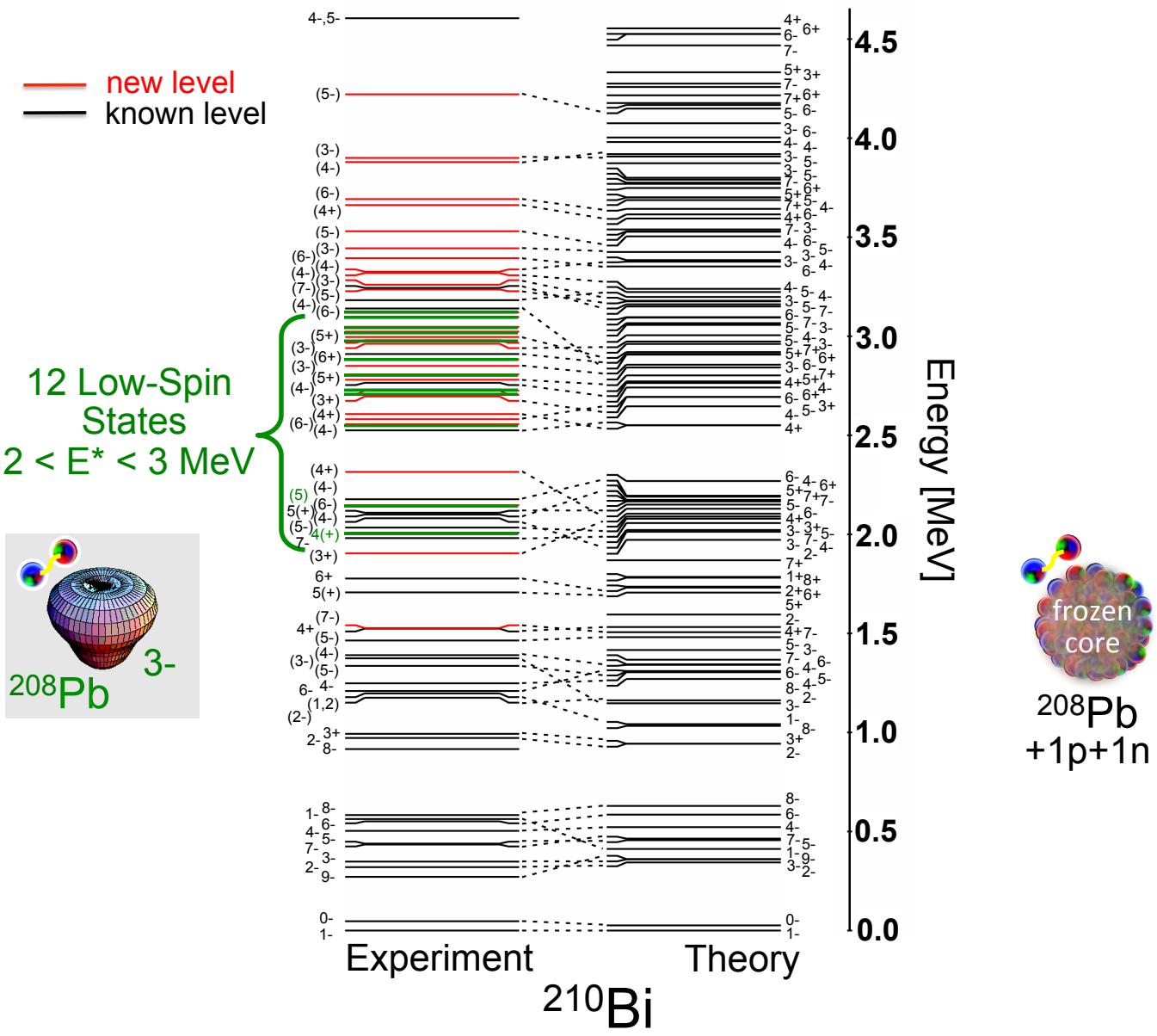

Fig. 6. Comparison between the experimental level scheme of ^{210}Bi, from cold neutron capture studies [73,74], and Shell model predictions with the OXBASH code, considering excitations of the proton- and neutron-valence particles only (as schematically illustrated in the cartoon on the right). The 12 states experimentally observed in the 2-3 MeV region, not described by the calculations, are marked in green on the left of the figure. They have no spin-parity assignment (apart from the two lowest-lying) and they are suggested to arise from the coupling between the ^{208}Pb octupole phonon and the proton-neutron valence particles, as illustrated by the cartoon on the left.

11. G.F. Bertsch, P.F. Bortignon, R.A. Broglia, C.H. Dasso, Phys. Lett. B80, 161 (1979).
12. P.F. Bortignon, R.A. Broglia, Nucl. Phys. A371, 405 (1981).
13. G.F. Bertsch, P.F. Bortignon, R.A. Broglia, Rev. Mod. Phys. 55, 287 (1983).
14. P.F. Bortignon, R.A. Broglia, G.F. Bertsch, Nucl. Phys. A460, 149 (1986).
15. P.F. Bortignon, A. Bracco, and R. A. Broglia, *Giant Resonances: Nuclear Structure at Finite Temperature* (Harwood Academic, New York, 1998).
16. V.Yu. Ponomarev, P.F. Bortignon, R.A. Broglia, and V.V. Voronov, Phys. Rev. Lett. 85, 1400 (2000).
17. T. Aumann, P.F. Bortignon, H. Emling, Ann. Rev. Nucl. Part. Sci. 48. 351 (1998).
18. R.A. Broglia, G. Colò, G. Onida and H. E. Roman, *Solid State Physics of Finite Systems* (Springer 2004).
19. M. Baldo and P.F. Bortignon, Lettere al Nuovo Cimento 14, 587 (1975).
20. M. Baldo, P.F. Bortignon, G. Colò, D. Rizzo, L. Sciacchitano, J. Phys. G: Nucl. Part. Phys. 42 (2015) 085109.

21. G. Colò, N. Van Giai, P.F. Bortignon, R.A. Broglia, Phys. Rev. C50 (1994) 1496.
22. G. Colò, H. Sagawa, and P.F. Bortignon, Phys. Rev. C82, 064307 (2010).
23. Y. F. Niu, G. Colò, and E. Vigezzi, Phys. Rev. C90, 054328 (2014).
24. Y.F. Niu et al., Phys. Rev. Lett. 114, 142501 (2015).
25. G. Colò, P. F. Bortignon, and G. Bocchi, Phys. Rev. C 95, 034303 (2017).
26. D. Lacroix, 2009 International Joliot-Curie School (EJC2009), arXiv:1001.5001[nucl-th].
27. SciDAC Review 6, 42 (2007).
28. S. Bottoni, G. Colò, and P.F. Bortignon, submitted to Phys. Rev. C.
29. J. Rowe, J. Math. Phys. 10, 1774 (1969).
30. G. Bocchi et al., Phys. Rev. C **89**, 054302 (2014).
31. C.R. Niţă et al., Phys. Rev. C **89**, 064314 (2014).
32. M. Asai et al., Phys. Rev. C62, 054313 (2000).
33. D. Bucurescu, M. Ivascu, G. Semenescu, and M. Titirici, Nucl. Phys. A189, 577 (1972).
34. R. M. Britton and D. L. Watson, Nucl. Phys. A272, 91 (1976).
35. B. G. Harvey et al., Nucl. Phys. 70, 305 (1965).
36. A. L. McCarthy and G. M. Crawley, Phys. Rev. 150, 935 (1966).
37. Y. Iwasaki et al., Phys. Rev. C 20, 861 (1979).
38. A. A. C. Klaasse and V. Paar, Nucl. Phys. A297, 45 (1978).
39. A.G. Hartas et al., Nucl. Phys. A279, 413 (1977).
40. R.H. Speak, At. Data Nuc. Data Tab. 42, 55 (1989).
41. D. Bucurescu et al., Nucl. Instrum. Methods Phys. Res. A 837, 1 (2016).
42. C.J. Chiara et al., Phys. Rev. C 85, 0234309 (2012).
43. G. Colò et al., Nucl. Phys. A 788, 173c (2007).
44. G. Colò et al., Comput. Phys. Commun. 184, 142 (2013).
45. B. A. Brown, Phys. Rev. C 58, 220 (1998).
46. E. Chabanat, P. Bonche, P. Haensel, J. Meyer, and R. Schaeffer, Nucl. Phys. A 643, 441 (1998).
47. S. Leoni et al., Phys. Rev. Lett. 118, 162502 (2017).
48. A. I. Morales et al., Phys. Lett. B 765, 328 (2017).
49. C. J. Chiara et al., Phys. Rev. C 86, 041304(R) (2012).
50. C. J. Prokop et al., Phys. Rev. C 92, 061302(R) (2015).
51. R.A. Einstein et al., Phys. Rev. 188,(1969)1815.
52. D. Montanari et al., Phys. Lett. B 697 (2011) 288.
53. D. Montanari et al., Phys. Rev. C 85, 044301 (2012).
54. D. Montanari et al., Phys. Rev. C 84, 054613 (2011)
55. Nuclear Data Base, http://www.nndc.bnl.gov/nudat2/
56. R. Broda, J. Phys. G: Nucl. Part. Phys. 32 (2006) R151.
57. A.M. Stefanini, et al., Nucl. Phys. A 701 (2002) 217c.
58. D. Montanari, et al., Eur. Phys. J. A 47 (2011) 4.
59. A. Gadea, et al., Eur. Phys. J. A 20 (2004) 193.
60. S. Bottoni et al., submitted to Phys. Rev. C.
61. G. Bocchi et al., Acta Phys. Pol. B46 (2015)647.
62. S. Bottoni et al., EPJ Web Conf. 193, 05001 (2018).
63. N. Cieplicka-Orynczak et al., Acta Phys. Pol. B48 (2017) 577.
64. S. Paschalis et al., Nucl. Instrum. Methods Phys. Res. A 709, 44 (2013).
65. H. L. Crawford, et al., Phys. Rev. C 95, 064317 (2017).
66. A. Gade et al., Phys. Rev. C 93, 031601 (2016).
67. P. Bhattacharyya, et al., Phys. Rev. Lett. 87 (2001) 062502.
68. D. Rosiak et al., Phys. Rev. Lett.121, 252501 (2018).
69. G. Bocchi et al., Phys. Lett. B760 (2016) 273.
70. S. Bottoni at al., Acta Phys. Pol. B50 (2019) 285.
71. M. Jentschel et al., Journ. Inst. 12 (2017) 11003.
72. J. R. Erskine, W.W. Buechner, and H. A. Enge, Phys. Rev. 128, 720 (1962).
73. N. Cieplicka-Orynczak et al., Phys. Rev. C 93, 054302 (2016).
74. N. Cieplicka-Orynczak et al., Phys. Rev. C 94, 014311 (2016).
75. B.A. Brown et al., MSU-NSCL report number 1289 (unpublished).
76. G. Herling and T.T. S Kuo, Nucl. Phys. A 181, 113 (1972).